

# Simulation supported POD curves for automated ultrasonic testing of pipeline girth welds

B. Chapuis · F. Jenson · P. Calmon · G. DiCrisci ·  
J. Hamilton · L. Pomié

Received: 15 November 2013 / Accepted: 7 March 2014 / Published online: 13 April 2014  
© International Institute of Welding 2014

**Abstract** A probability of detection (POD) curve relates the detectability of a flaw to its size. It plays an important role in the qualification process of nondestructive testing (NDT) methods since it gathers the influence of all the parameters that can alter the detectability of the flaw and, therefore, gives a measure of the performance of the NDT method (in terms of detection capabilities). POD curves were before exclusively obtained thru expensive and time consuming experimental campaigns. Simulation based POD calculations have recently been introduced in the NDT community. The determination of POD curves based on the simulation of the inspection method is presented in the case of the automated ultrasonic (AUT) inspection of girth welds using the zonal discrimination approach. The methodology to obtain these curves is divided into different steps that are derived from the ASTM standard practices and Det Norske Veritas (DNV) recommendations for these AUT inspection procedures using hit/miss analysis. The simulations and the computation of the POD curves are performed using the software CIVA developed by the CEA-LIST.

**Keywords** Nondestructive testing · Circumferential welds · Pipelines · Reliability · Ultrasonic testing

## 1 Introduction

Pipelines are generally constructed by welding two pipes together, through a girth weld. The inspection of these girth welds has been commonly performed for years using

automated ultrasonic (AUT) systems which ensure a very good productivity. These systems are composed of several transducers which allow, using the zonal discrimination approach, a complete examination of the weld with a single scan along the circumference of the pipe.

However, the use of these systems is subjected to the demonstration of their performance confronted to realistic degradations of their environment. This demonstration is synthetized in a qualification dossier and is supported by experimental sensitivity analysis to several key factors (temperature, positioning of the probes, etc.) [1]. These sensitivity analysis are performed using a systematic probability of detection (POD) approach, and requires a large amount of experiments which are often long and costly. We present here a modeling of a typical AUT inspection of girth weld using the CIVA software developed by the CEA-LIST and its POD module. CIVA allows determining POD curves based on the simulation of the inspection method and the description of the uncertainties associated with the procedure (probe positioning, pipe thickness variations from one weld to another, etc.). These curves can be used in several ways such as optimizing the trials to perform during an experimental campaign of POD curves determination or providing technical justifications when minor changes in the inspection procedure occur in order to avoid a new experimental campaign. Simulation-supported POD curves can also allow assessing cases for which experiments have limitations for example the manufacturing of small size realistic defects.

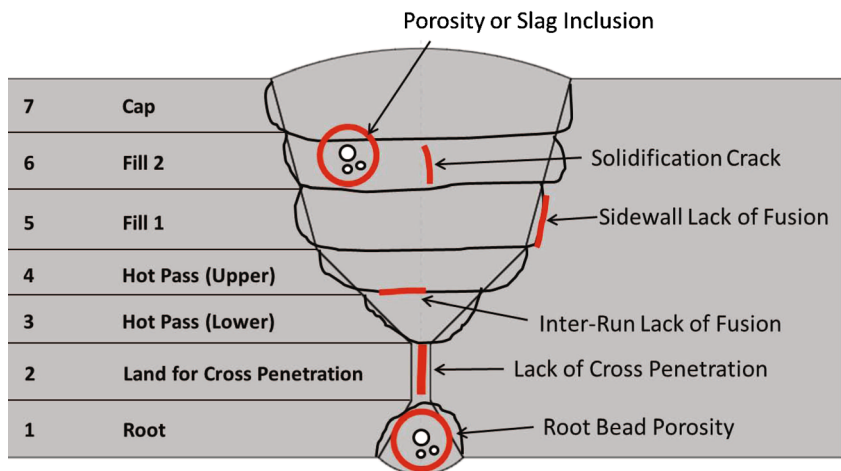
## 2 AUT and zonal discrimination approach

The zonal discrimination approach, used by AUT systems dedicated to girth welds inspection, is described in the ASTM E1961 standard practice [2]. It consists of dividing the thickness of the pipe wall in different zones of 1–3 mm height

B. Chapuis (✉) · F. Jenson · P. Calmon  
CEA-LIST, Centre de Saclay, 91191 Gif-sur-Yvette, France  
e-mail: bastien.chapuis@cea.fr

G. DiCrisci · J. Hamilton · L. Pomié  
Technip, 75773 Paris, France

**Fig. 1** Typical division of the weld in zones and kind of researched defects



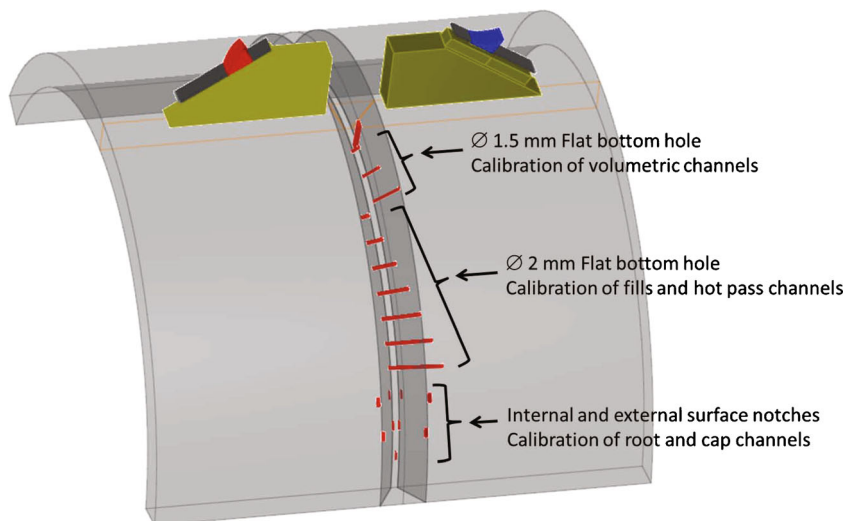
corresponding approximately to the weld pass thickness (Fig. 1). Each zone is inspected using a dedicated ultrasonic beam directed at a fixed position. This allows to locate the depth of the defect and to give an approximation of its height.

The amplitude of the echo measured from a real defect during the girth weld inspection is then compared to that of the calibrated reflectors (flat bottom holes or notches). The calibration procedure, i.e., the measurement of these calibrated amplitudes, is therefore a crucial point of the technique. For that purpose, a calibration block is manufactured and scanned before and after each weld inspection to ensure the correct set-up of the inspection system (Fig. 2).

**3 Modeling of the calibration block inspection**

The geometry of the weld considered in this paper is described in Fig. 3, it is considered as an isotropic material with the same

**Fig. 2** Example of calibration block



properties than the base material. The following material parameters have been used in the simulation:

- Longitudinal wave velocity=5,900 m/s,
- Transversal wave velocity=3,230 m/s ,
- Density=7.8 g/cm<sup>3</sup>.

The V bevel is inspected by a 7.5-MHz phased array probe composed of 60 elements. The inspection of the calibration block using the probe on the upstream side of the weld is presented in Fig. 4. The different channels necessary for the zonal discrimination method are obtained using different elements in emission and reception and different delay laws. An example of delay law for one channel and the corresponding ultrasonic ray path is presented in Fig. 5.

The simulation of the scan of the calibration block with the different channels, using a similar methodology than in references [3, 4], is presented in Fig. 6. Each line corresponds to the echodynamic curve of the channel, i.e., the maximal

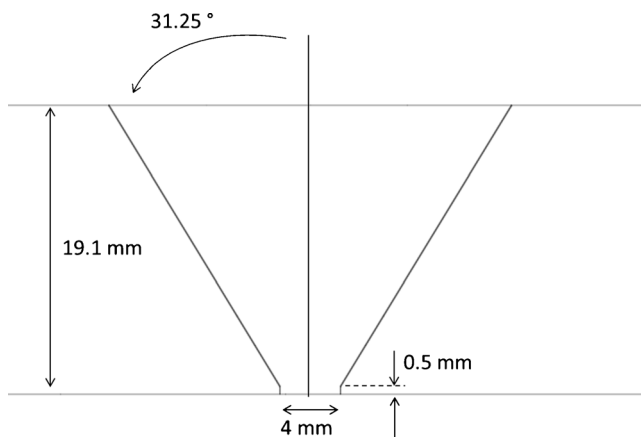


Fig. 3 Dimensions of the V bevel considered in this paper

amplitude of the signal measured for each position of the scan path. Colors are used to highlight the positions for which the signal reaches some amplitude thresholds. We can observe for each channel, as expected, a peak of the response for the position of the corresponding calibration reflector of the channel. With respect to the standard practice ASTM E1961-11, the gain for each simulated channel is adjusted to set the amplitude of the calibration reflector to 80 % full screen height (FSH). For symmetry reasons, only the calibration of the upstream channels has been simulated.

#### 4 Physical meanings of POD curves and CIVA POD module

The probability of detection (POD) curve for an AUT system is defined as:

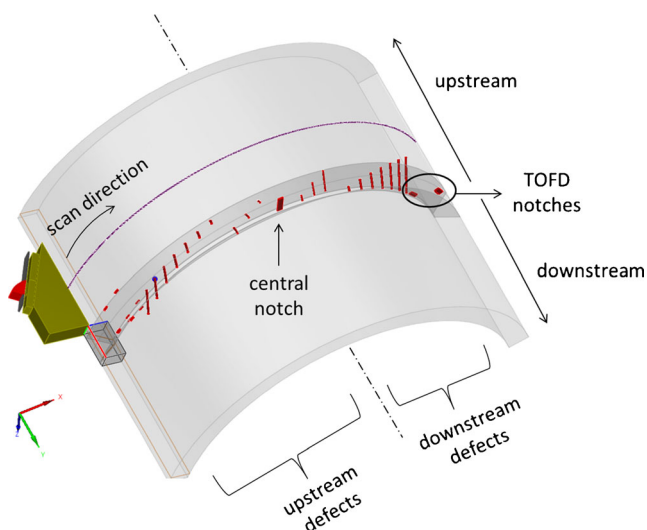


Fig. 4 Inspection of the calibration block from the upstream side

the curve describing the probability that, given a defect height, the AUT system gives a signal above a defined threshold.

In a deterministic approach, the signal given by the AUT system is a function (generally growing) of the defect height. However, in reality, when the responses are measured for different defects, with different operators, on different samples, a scattering is observed around this “ideal” linear function (Fig. 7). This is the consequence of several parameters that are called “influencing parameters”.

The influencing parameters are classically divided into two categories: the application parameters (that are linked to the physical behavior of the NDT system) and human factors (fatigue, operator skill level, access conditions, etc.). For AUT systems, the application parameters are essentially:

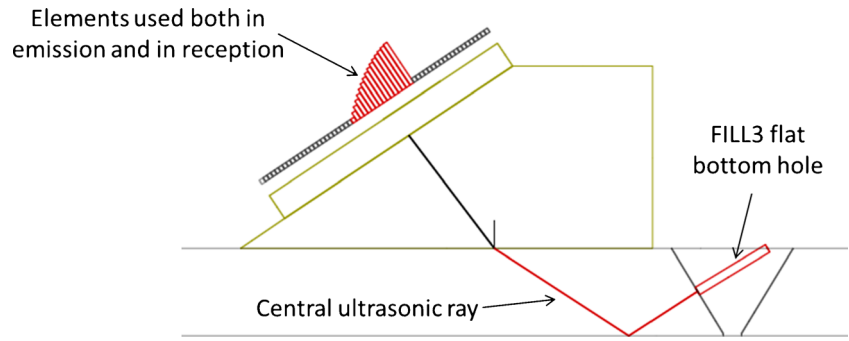
- material parameters (wave velocities, density, microstructure)
- geometry of the specimen
- surface roughness
- location of the flaw
- orientation and geometry (shape, surface roughness) of the flaw
- the orientation and wedge geometry of the probe
- the scan parameters (sampling, positioning of the probe, etc.)

Human factors are difficult to model and their influence is generally not taken into account in simulation studies, they have neither been included here. However, works are carried out on this aspect which may allow us to incorporate it in the future [5].

The fluctuations around the deterministic response of the NDT system are the source of the POD curve, as explained on Fig. 8. For the range of defect for which all the signal are below the threshold (zone 1) the POD is 0, no defect of these sizes are detected. For the range of defect for which all the signal are above the threshold (zone 2) the POD is 1, all the defect of these sizes are detected. The intermediate range of defect height is a transition zone (zone 3), on which the POD curve increases from 0 to 1. The shape of the POD curve is strongly linked to the fluctuations of the signal around the detection threshold.

Two curves are always given on a POD graph. The left one, in blue on Fig. 8, is the POD curve. The defect height for which this curve reaches the values 0.9 is called  $a_{90}$ , which the defect height detected 90 % of the time. However, the POD curve is only an estimated curve, since it is determined with a limited number of experiments and

**Fig. 5** Example of focal law for the inspection of FILL3 channel



samples (or simulations). The second curve (in red on Fig. 8) indicates therefore the (conservative) confidence on the estimation of the POD curve: there are 95 % chances that the true POD curve is on the left of this curve. The defect height for which this curve reaches the values 0.9 is called  $a_{90/95}$ . In practice,  $a_{90/95}$  is the value used to characterize the performances of the NDT system. Since  $a_{90/95}$  is always higher than  $a_{90}$ , it is therefore a conservative value.

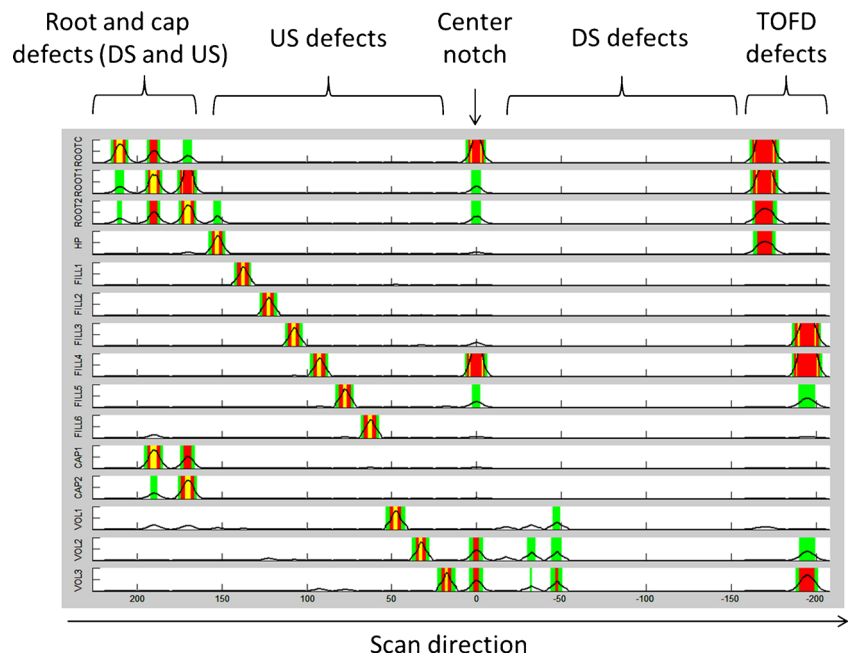
Since version 10, CIVA software has a module dedicated to the computation of POD curves. The determination of purely numerical POD curves in CIVA is based on uncertainties propagation (Fig. 9): the uncertainties on the input parameters (for example the exact wave velocity in the sample is not known or the position of the probe is given with a tolerance) are taken into account to determine the variability that it can induce on the response of the NDT system.

After the definition of the configuration (specimen dimensions, probe characteristics and positioning, defect), the first step of the simulation of POD curves using CIVA consists in describing the sources of fluctuation, i.e., the uncertainties on the input parameters. This is done using statistical distributions that describe each influencing parameter (Fig. 10).

A large number of configurations with different values of the uncertain parameters are then simulated, and the results are presented in a window similar to that given in Fig. 11. A table summarizes the different configurations that have been simulated with the corresponding values of the uncertain parameters. A first graph presents the signal amplitude responses of the simulated configurations, as a function of the defect height. A second graph presents the POD curve for the given threshold.

According to the recommended practices for AUT of pipeline girth welds [6, 7], the POD curve is determined through a

**Fig. 6** Echodynamics for the inspection of the calibration block with different upstream channels. Color code: *green* amplitude > 20 % FSH, *red* amplitude > 40 % FSH, *yellow* amplitude ∈ [70 %; 99 %] FSH



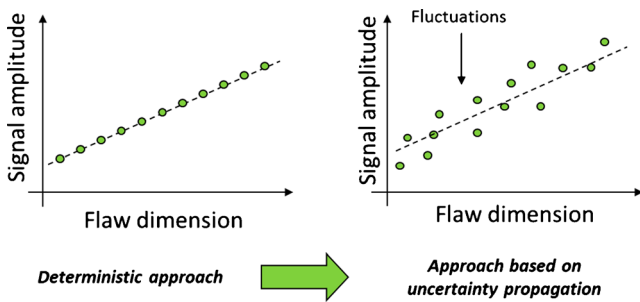


Fig. 7 Scattering of the signal response around the deterministic response of the NDT system

hit/miss analysis of the simulated results with a cumulative lognormal distribution function or the log odd model, which is very close to it, for curve fitting. In this paper, the cumulative lognormal distribution function is used. The detection threshold is set to 20 % FSH for the curves presented in this paper but this value can be modified in the graphical user interface.

### 5 Simulation supported POD curves for AUT inspection of girth welds

The POD is computed for a rectangular defect 15 mm long. The following channels have been simulated:

- CAP1
- FILL6
- FILL5
- FILL4
- FILL3
- FILL2
- FILL1
- HP
- ROOT

The selected influential parameters have been:

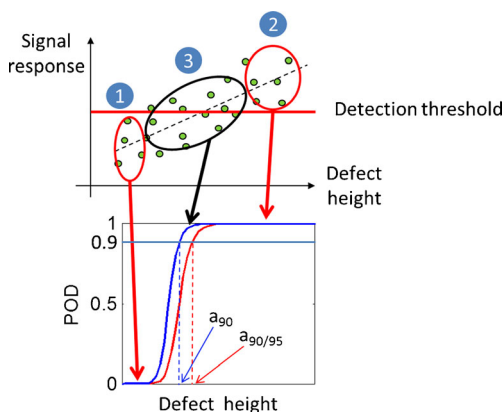


Fig. 8 Hit/miss analysis of signal response data and POD curve

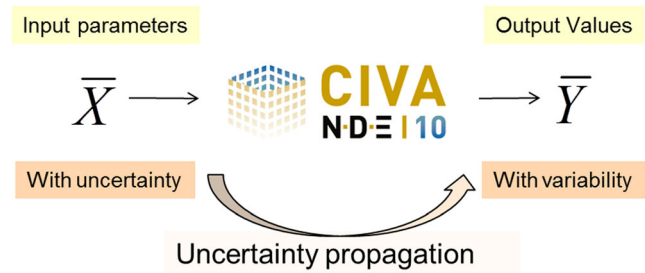


Fig. 9 Uncertainty propagation in CIVA POD module for the simulation of POD curves

- Pipe thickness
- Position of the guide-band of the AUT system
- Skew of the guide-band
- Tilt of the defect
- Position of the defect
- Hi-Lo (misalignment) of the pipe

After analysis of geometrical data on real pipes (pipe thickness and internal diameter measurements), a normal distribution with  $\mu=19.1$  mm and  $\sigma=0.3$  mm, has been chosen for describing the pipe thickness variations (Fig. 10).

According to the AUT procedure a 1 mm tolerance is allowed on the offset of the guide-band. A uniform distribution of  $\pm 1$  mm around the nominal position of the guide-band has therefore been chosen to describe the uncertainty on this parameter. The skew of the guide-band has been estimated to be correctly represented by a uniform distribution of  $\pm 0.3^\circ$ .

The defect is positioned for each channel along the bevel with a tilt of  $\pm 1.5^\circ$  with respect to the bevel and  $\pm 1$  mm from the nominal position. Uniform distributions have been used to describe these uncertainties since no prior information are available on these parameters. The center of the defect is randomly located in the zone defined by the zonal discrimination approach.

For geometrical reasons, the Hi-Lo is an influent parameter only for ROOT channel. It has been modeled here as a random misalignment of the two pipes, of  $\pm 1.5$  mm (Fig. 12).

Since the probes of an AUT system are highly focused (which is necessary for the zonal discrimination) and due to the uncertainties on some input parameters (for example probe positioning), a defect in a given zone might not be detected anymore by the nominal probe but a probe adjacent to the nominal one. The determination of the “true” POD curve for one channel requires therefore the simulation of the different configurations for the nominal probe (and associated delay laws if applicable) and the simulation of the response of the adjacent probes with the same configurations (same pipe geometry, defect position etc.). The hit/miss analysis is performed on the results of the whole set of simulations (some “misses” of the nominal channels are transformed into “hits”



**Fig. 10** CIVA GUI tab for the description of the influencing parameters using statistical distributions

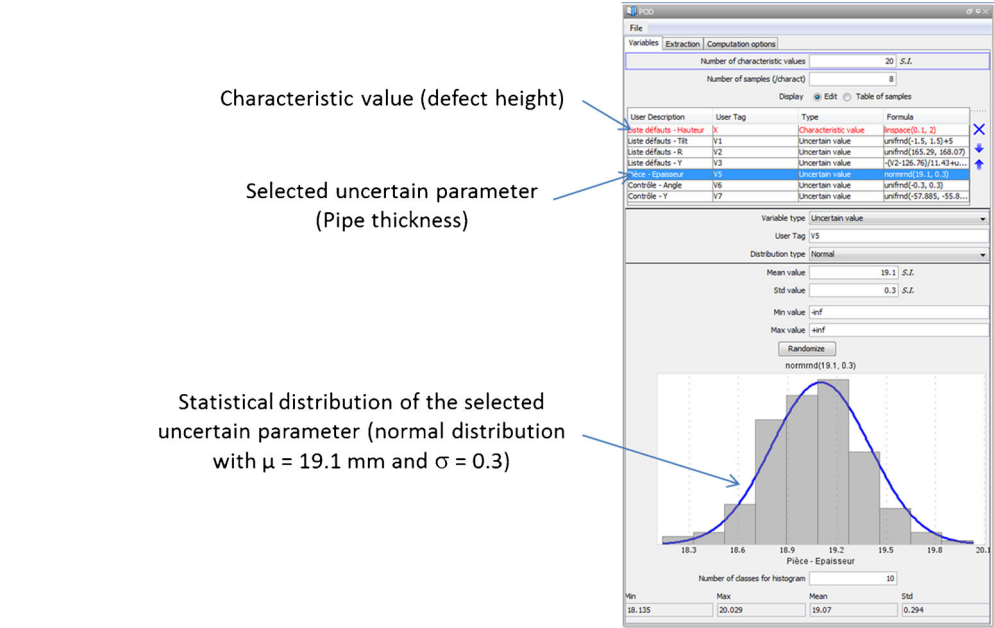


**Fig. 11** CIVA analysis window for POD curve computation results

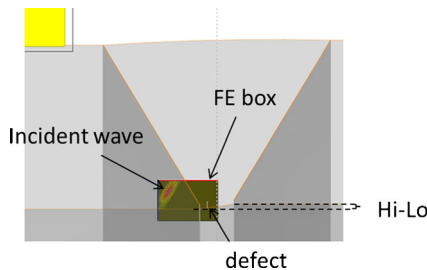
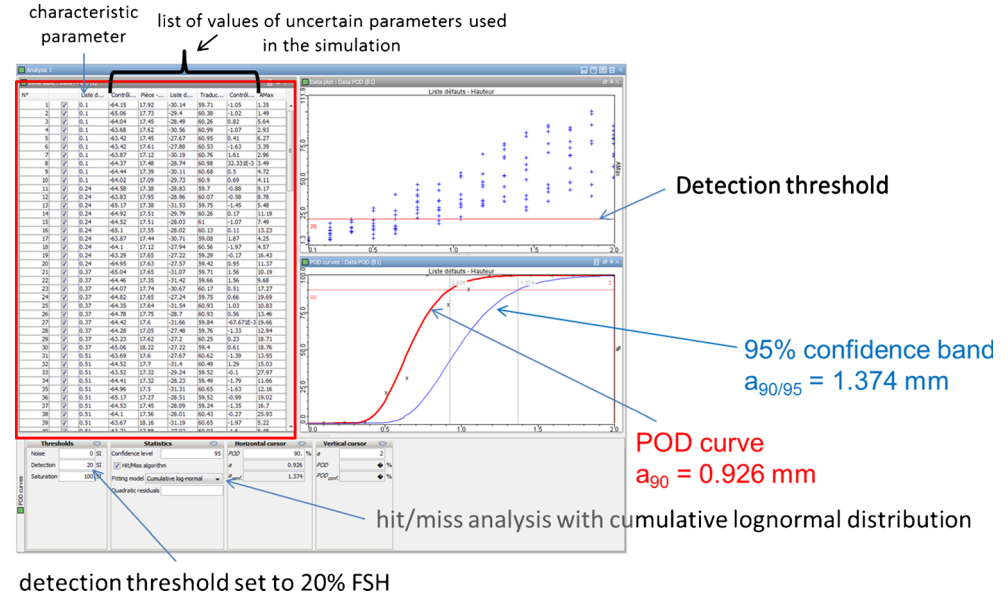
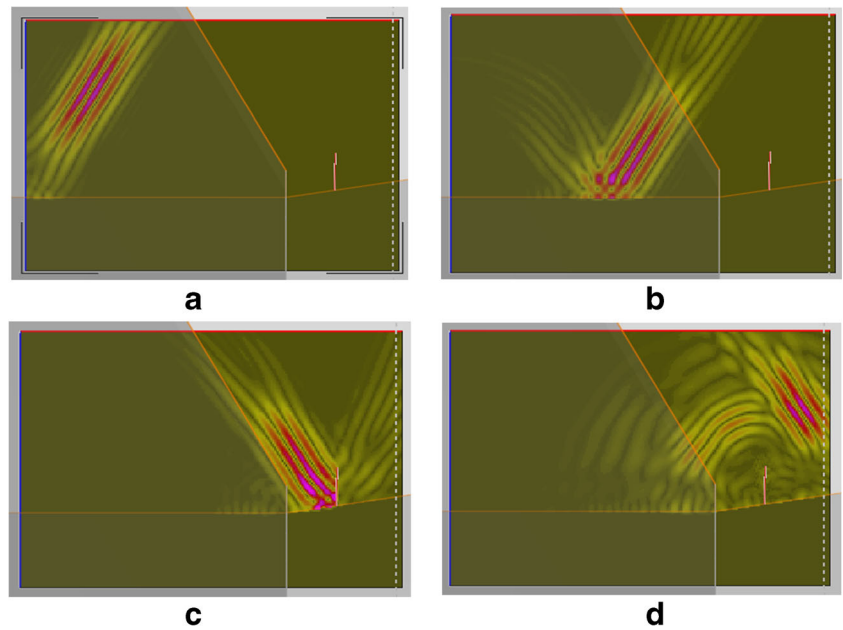


**Fig. 12** Defect response computation using Athena module of CIVA for ROOT channel: a finite element box is placed around the defect, the incident ultrasonic field on the box is calculated by CIVA

thanks to the adjacent channels) to determine the POD curve of the nominal channel.

The simulations for the ROOT channel highlighted a limitation of the current semi-analytical models implemented into CIVA: when the Hi-Lo is positive (case of Fig. 12), two different contributions are incident on the defect at the same time, which leads to numerical errors. For the ROOT channel only, the CIVA simulations have therefore been assisted with the finite element module Athena, which is fully integrated into CIVA

**Fig. 13** Snapshots of the interaction of the incident wave with a defect at the root with Hi-Lo



since version 11. This module computes the response of the defect thanks to a 2D finite element box placed around it (Fig. 12). Since the length of the defect is significantly larger than the focal spot, the 2D approximation is valid. The incident ultrasonic field on the finite element box is calculated by CIVA and is then propagated into the box through finite elements modeling. This strategy exploits the power of finite elements in terms of complexity of defect

shape and position that can be addressed and the speed of the semi-analytic models of CIVA since the size of the finite element is limited to its minimum. Since Athena is integrated into CIVA GUI, the coupling between the incident field and the finite element box is automatic and completely transparent for the user. The only difference from CIVA “classical” models from a user point of view is the computational time which is increased.

**Fig. 14** Simulated POD curve for the channel FILL5, taking into account the adjacent channels

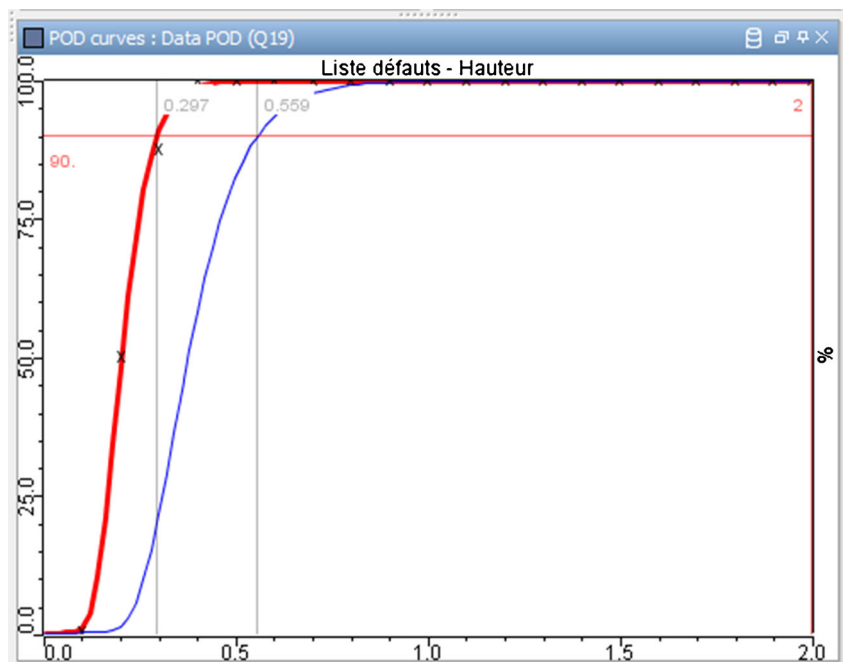
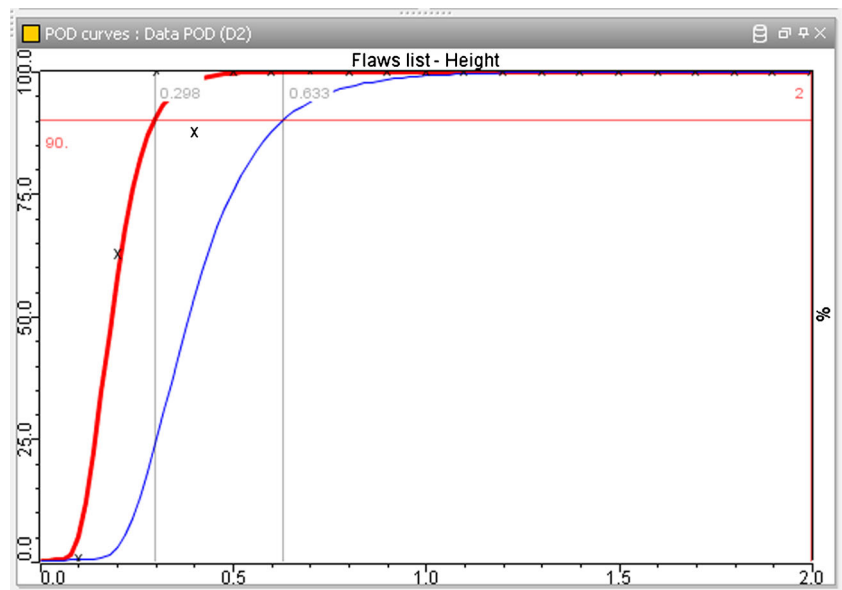


**Fig. 15** Simulated POD curve for the channel ROOT, taking into account the adjacent channels



One of the advantages of the finite elements box is the possibility to visualize the propagation of the ultrasonic field in the box and its interaction with the defect which can be very useful to understand the physical phenomena that can be involved and could lead to optimization of the inspection procedure (Fig. 13).

Examples of POD curves determined by CIVA for two channels are given in Figs. 14 and 15 for channels FILL5 and ROOT, respectively.

A synthesis for all the channels is presented in Table 1. The values  $a_{90/95}$  obtained for the different channels are very similar, we can conclude that the detection of a 15-mm long planar defect along the weld bevel is almost uniform through the thickness of the pipe. These values cannot be considered as definitive values of the system's performance, since the human factors have not been taken into account in the analysis. This should be completed and validated by experiments to give the "real" POD curve. However, since with such AUT system the inspection is automated, human factor influence is expected to be very low.

**Table 1** Synthesis of the POD curves simulations channel by channel

	$a_{90}$ (mm)	$a_{90/95}$ (mm)
ROOT	0.3	0.6
HP	0.2	0.6
FILL1	0.3	0.8
FILL2	0.3	0.5
FILL3	0.3	0.6
FILL4	0.3	0.6
FILL5	0.3	0.6
FILL6	0.4	0.6
CAP1	0.2	0.5

## 6 Conclusion

We have presented in this paper an example of POD curves determined through the simulation of the automated ultrasonic inspection of a girth weld. The procedure of the inspection is derived from the ASTM standard practices and DNV recommendation. A first step consisted in simulating the inspection of the calibration block used to define reference amplitude threshold for the detection of the defects. The different channels of the AUT system have been considered. Then, the POD curves for the different channels have been determined, taking into account cases for which, due to the uncertainties on the input parameters, the defect is not detected anymore by the nominal channel but by an adjacent one.

These simulation-supported POD curves can be used in several ways:

- Optimizing the design of experiments: select the trials (manufactured defects) in order to focus on the range of interest of the POD curve (reduce number of tests in ranges where  $POD=0$  or  $1$ )
- Quantify the impact of an uncertain parameter not taken into account in an existing POD curve
- Identify the uncertain parameters to better control to bring back a POD curve to an acceptable value
- Provide technical justifications when minor changes of the procedure are carried out in order to avoid a new experimental campaign
- Design an inspection procedure with an objective in terms of POD
- ...



## References

1. DNV-OS-F101 (2010) Submarine pipeline systems, Appendix E “Automatic ultrasonic girth weld testing”
2. ASTM E1961-11 (2011) Standard practice for mechanized ultrasonic testing of girth welds using zonal discrimination with focused search units
3. Ginzel E, Stewart D (2011) CIVA Modelling for pipeline zonal discrimination, NDT.net
4. Foucher F, Dubois P, Gaffard V, Godinot H, Romazzotti H, Courbot A, Schumacher E (2012) Validation of the simulation of pipeline girth welds PA UT inspections, Proceedings of the ASNT Fall Conference
5. Forsyth D, Aldrin J (2009) Build Your Own POD, Proceedings of the 4th European-American Workshop on Reliability of NDE
6. NordTest Technical Report 394 (1998) Guidelines for NDE reliability determination and description
7. DNV-RP-F118 (2010) Pipe girth weld AUT system qualification and project specific procedure validation